Neoplasma 2023; 70(3): 375–389

doi:10.4149/neo_2023_230418N216

Topical application of local anesthetics to melanoma increases the efficacy of anti-PD-1 therapy

Miroslav TIBENSKY[1,2,#], Filip BLASKO[1,2,#], Peter VARGOVIC[2], Jana JAKUBIKOVA[3], Dana CHOLUJOVA[3], Jana JAKUBECHOVA[3], Boris MRAVEC[1,2,*]

[1]*Institute of Physiology, Faculty of Medicine, Comenius University Bratislava, Bratislava, Slovakia;* [2]*Biomedical Research Center, Institute of Experimental Endocrinology, Slovak Academy of Sciences, Bratislava, Slovakia;* [3]*Biomedical Research Center, Cancer Research Institute, Slovak Academy of Sciences, Bratislava, Slovakia*

**Correspondence: boris.mravec@fmed.uniba.sk*
#Contributed equally to this work.

Received April 18, 2023 / Accepted June 9, 2023

Experimental and clinical data have shown that the nervous system can significantly stimulate the initiation and progression of melanoma. In support of this, approaches that reduce the transmission of signals from peripheral nerves to effector tissues reduce the recurrence of melanoma. Therefore, we investigated the effect of topical application of the local anesthetic Pliaglis (7% lidocaine and 7% tetracaine) on the growth of melanoma induced by intradermal application of B16F0 cells in mice without treatment and in mice treated with the anti-PD-1 antibody. We found that application of Pliaglis to melanoma significantly reduced its growth and this effect was even pronounced in mice treated with the anti-PD-1 antibody. To determine the mechanisms and pathways responsible for the observed effect, the *in vitro* effect of incubating melanoma cells with lidocaine and/or tetracaine and the *in vivo* gene expression of cancer and immune-related factors, percentage of immune cells, gene expression of selected neurotransmitter receptors and nerve growth factors in melanoma tissue were studied. We found that lidocaine and tetracaine significantly reduced the viability of B16F0 cells *in vitro*. In mice with melanoma, Pliaglis potentiated the effect of anti-PD-1 antibody on gene expression of COX-2, IL-1β, IL-6, CCL11, F4/80, CD206, and NCR1. In addition, Pliaglis increased the gene expression of α9nACHR and 5-HT2a receptors and decreased the gene expression of nerve growth factor receptor (p75NTR) and p53. We also observed Pliaglis-mediated changes in myeloid populations. Topical application of this local anesthetic cream decreased the $CD11b^{+}Gr1^{-}$ population and increased the $CD11b^{+}Gr1_{high}$ population. Our data suggest that Pliaglis reduces melanoma growth through a direct effect on melanoma cells as well as through modulation of the immune response. The involvement of nervous system-related signaling in the inhibitory effect of Pliaglis on melanoma is inconclusive from our data.

Key words: B16F0 cells; immune system; lidocaine; melanoma; neurobiology of cancer; tetracaine

Data accumulated over the past two decades have clearly demonstrated that the nervous system plays an important role in the initiation and progression of cancer, including melanoma [1]. In support of this, research in cancer neurobiology has shown that the modulation of signals transmission from the nervous system to the tumor macro- and micro-environment can significantly affect the course of cancer. The effect of the nervous system on cancer is mediated by both humoral and neural pathways [2]. Signals transmitted by neural pathways to cancer tissue are experimentally modulated by molecules that bind to neurotransmitter receptors. For example, the stimulatory effect of sympathetic nerves on cancer can be reduced by β-blockers (e.g., propranolol) [3]. This approach is beginning to be used experimentally for the treatment of several cancers, including those located in visceral organs. Importantly, the prospective study [4] showed that the off-label use of propranolol significantly reduced melanoma recurrence in patients. However, the superficial localization of melanoma creates the basis for another approach to reduce the transmission of nerve signals to the cancer tissue, specifically the topical application of anesthetics. Therefore, we focused in our experiment on investigating the effect of reducing the signal transmission through nerves in melanoma and its close vicinity by topical anesthetic application on melanoma growth.

When the anesthetic is applied to the skin, it reduces the transmission of action potentials through the periph-

eral nerves. Therefore, it may also reduce the transmission of nerve signals within the cancerous tissue. This effect may be mediated by inhibition of axonal reflex activity in sensory nerve fibers within the melanoma, as well as by reduction of signals transmitted by sympathetic fibers from the spinal cord to the melanoma and surrounding tissues.

Therefore, to test the effect of local anesthetics on melanoma growth, we repeatedly administered Pliaglis, a local anesthetic containing 7% lidocaine and 7% tetracaine, topically to melanomas induced by intradermal application of B16F0 cells in mice. We administered Pliaglis to mice with melanoma without any other treatment, as well as to mice treated with the conventional oncological treatment of melanoma using the anti-PD-1 antibody. Since we observed an inhibitory effect of Pliaglis on melanoma growth, we focused on elucidating the mechanisms responsible for the observed effect. Therefore, we performed *in vitro* incubation of B16F0 cells with lidocaine and/or tetracaine. In addition, we determined in mouse melanoma tissue gene expression of cancer-related factors such as p53, pro- and anti-inflammatory factors, cancer-related immune factors, percentage of immune cells in melanoma tissue, and gene expression of selected receptors for neurotransmitters and nerve growth factors.

Materials and methods

Experimental animals. The study was conducted in 8-week-old male mice (C57/BL/6J strain, Charles River, Germany). Mice were housed three or four per cage and maintained under standard laboratory conditions (12-hour light/dark cycle, lights on at 7:00 AM, ambient temperature 22±2 °C, and 55±10% humidity). Animals had *ad libitum* access to water and standard pelleted food. The experiment was approved by the Animal Care Committee of the Institute of Experimental Endocrinology, Biomedical Research Center, Slovak Academy of Sciences, Bratislava, Slovakia, and by the State Veterinary and Food Administration of the Slovak Republic (approval No. Ro-4302/18-221/3). The animals were cared for in accordance with the Guide for the Care and Use of Laboratory Animals published by the US National Institutes of Health.

Cell lines and reagents. The murine melanoma cell line B16F0 was used for the *in vivo* experiment. Cells were cultured in complete culture medium DMEM, supplemented with 10% fetal bovine serum and an antibiotic-antimycotic mixture (all purchased from Life Technologies) in a humidified atmosphere of 5% CO_2 at 37 °C.

A suspension of B16F0 melanoma cells was injected intradermally at a dose of 3×10^5 cells in 30 µL PBS. Vehicle ointment (4% methylcellulose) and Pliaglis anesthetic cream (containing 7% lidocaine and 7% tetracaine, the highest concentration of anesthetics approved by the FDA and EMA) were administered topically. Pliaglis anesthetic cream was kindly provided by Crescita Therapeutics. Therapeutic anti-PD-1 antibody [RMP1-14 (Rat IgG2a), purchased from BioXCell] was injected intraperitoneally at a dose of 250 µg/injection. The antibody was diluted to a therapeutic concentration with InVivoPure pH 7.0 Dilution Buffer (purchased from BioXCell).

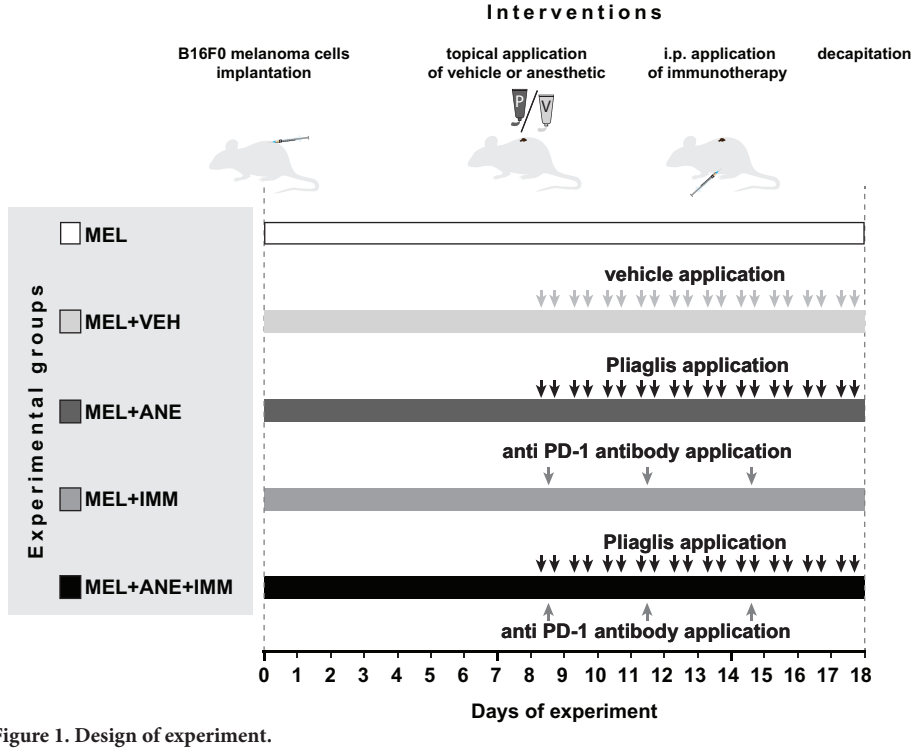

Figure 1. Design of experiment.

Cell viability assay. For the *in vitro* experiment, we used the murine melanoma cell line B16-F0 and the human melanoma cell line A375. Melanoma cells were plated in triplicate in a 96-well plate (3×10^3 cells/well) for each group. Plates were incubated overnight at 37 °C in a humidified atmosphere of 5% CO_2. The next day, the cells were exposed to lidocaine and tetracaine at a fixed concentration. After 72 h, the medium was replaced with CellTiter 96 Aqueous One Solution Cell Proliferation Assay (Promega) for 2 h and read out spectrophotometrically at 490 nm.

Design of *in vivo* experiment and treatment scheme. All animals were divided into five experimental groups (Figure 1): 1) MEL group – animals with intradermally injected melanoma cells; 2) MEL+VEH group – animals with intradermally injected melanoma cells and topically administered vehicle ointment on the surface of the melanoma; 3) MEL+ANE – animals with intradermally injected melanoma cells and topically administered Pliaglis anesthetic cream on the surface of the melanoma; 4) MEL+IMM – animals with intradermally injected melanoma cells and intraperitoneally administered anti-PD-1 antibody; 5) MEL+ANE+IMM – animals with intradermally injected melanoma cells and combined treatment with Pliaglis and anti-PD-1 antibody.

The experiment with intradermal administration of B16F0 tumor cells lasted 18 days and treatment started on day 8. Topical application of Pliaglis or the ointment vehicle was performed twice daily at least 8 h apart. On days 8, 11, and 14, mice from the MEL+IMM and MEL+ANE+IMM groups received anti-PD-1 antibody intraperitoneally. The experiment was terminated by decapitation. Subsequently, the tumor mass was removed and weighed. The tumor was removed, the tissue obtained was used for flow cytometry and the rest of the tissue was frozen until further analysis of gene expression.

RNA isolation and RT-PCR. All steps related to RNA isolation, reverse transcription of RNA, and real-time PCR were performed as previously described by Tillinger et al. [5]. The primer sequences are listed in Table 1. The obtained data were normalized to glyceraldehyde-3-phosphate dehydrogenase levels and expressed as the relative fold change calculated by the ΔΔCt method according to Livak et al. [6]. Melting curve analysis was performed to confirm the specificity of the amplified products.

Flow cytometry analysis. Tumors were isolated and processed into a single-cell suspension according to Pachynski et al. [7]. Zombie NIR™ Fixable Viability Kit (Bio Legend) was used for live/dead discrimination according to the manufacturer's protocol. Cells were fixed with Foxp3/Transcription Factor Staining Buffer Set (Thermo Fisher Scientific) according to the manufacturer's protocol. Non-specific antibody binding was blocked with TruStain FcX™ antibody (BioLegend) and rat serum (Thermo Fisher Scientific). Antibodies against mouse CD45-PE Cy5 (30-F11 clone), CD3-FITC (17A2 clone), CD4-PE (GK1.5 clone), CD8-PE Cy7 (53-6.7 clone), CD11b-APC (M1/70 clone), Gr-1-BV510 (RB6-8C5 clone) were used for cell-surface staining (all purchased from BioLegend). Cells were washed, filtered again through a 70 μm cell strainer, and analyzed using a BD FACS Aria II SORP UV. Collected data were analyzed in FlowJo (Tree Star) and the representative gating

Table 1. Sequences of primers used for amplification of target cDNAs.

Gene name	Primer sequence
p75NTR	For. 5'-GGAGAGAAACTGCACAGCGACA-3' Rev. 5'-CAGGCTACTGTAGAGGTTGCCA-3'
CCL11	For. 5'-TGCAGAGCTCCACAGCGCTT-3' Rev. 5'-GGGTGAGCCAGCACCTGGGA-3'
TP53	For. 5'-GGCGTAAACGCTTCGAGATG-3' Rev. 5'-TTCAGGTAGCTGGAGTGAGC-3'
COX2	For. 5'-GTTCATCCCTGACCCCCAAG-3' Rev. 5'-TTAAGTCCACTCCATGGCCC-3'
IL-1β	For. 5'-TGCCACCTTTTGACAGTGATG-3' Rev. 5'-ATGTGCTGCTGCGAGATTTG-3'
IL-6	For. 5'-TCCGGAGAGGAGACTTCACA-3' Rev. 5'-TTGCACAACTCTTTTCTCATTTCCA-3'
IL-10	For. 5'-GTAGAAGTGATGCCCCAGGC-3' Rev. 5'-AATCGATGACAGCGTCGCA-3'
TNF-α	For. 5'-AGGCACTCCCCCAAAAGATG-3' Rev. 5'-CCATTTGGGAACTTCTCATCCC-3'
ADRB2	For. 5'-CAGAGCCTGCTGACCAAGAA-3' Rev. 5'-GGGGCACGTAGAAAGACACA-3'
NGF	For. 5'-GGCAGCATGGTGGAGTTTTG-3' Rev. 5'-TACGCTATGCACCTCACTGC-3'
CCL2	For. 5'-CCACAACCACCTCAAGCACT-3' Rev. 5'-AGGCATCACAGTCCGAGTCA-3'
F4/80	For. 5'-GGAGGACTTCTCCAAGCCTATT-3' Rev. 5'-AGGCCTCTCAGACTTCTGCTT-3'
FOXP3	For. 5'-CTGGACAACCCAGCCATGAT-3' Rev. 5'-ACATTGATCCCAGGTGGCAG-3'
IFN-γ	For. 5'-CGGCACAGTCATTGAAAGCC-3' Rev. 5'-TGTCACCATCCTTTTGCCAGT-3'
Ly-6C	For. 5'-ATCTGTGCAGCCCTTCTCTG-3' Rev. 5'-TCCCTGAGCTCTTTCTGCAC-3'
Ly-6G	For. 5'-TGCAGAAAGAGCTCAGGGG-3' Rev. 5'-CAGAGTAGTGGGGCAGATGG-3'
PRF1	For. 5'-TCTTGGTGGGACTTCAGCTT-3' Rev. 5'-TGCTTGCATTCTGACCGAGT-3'
TGF-β	For. 5'-TGGAGCAACATGTGGAACTC-3' Rev. 5'-GTCAGCAGCCGGTTACCA-3'
PD-L1	For. 5'-ACTTGCTACGGGCGTTTACT-3' Rev. 5'-GGGAATCTGCACTCCATCGT-3'
α9nAChR	For. 5'-AATGTGACCCTGGAGG-3' Rev. 5'-CACGTTGGTGCTGGC-3'
5-HT2a	For. 5'-CGTGTCCATGTTAACCATCC-3' Rev. 5'-TCAGGAAGGCTTTGGTTCTG-3'
NK-1R	For. 5'-CTTGCCTTTTGGAACCGTGTG-3' Rev. 5'-CACTGTCCTCATTCTCTTGTG-3'
VPAC1	For. 5'-GATGTGGGACAACCTCACCTG-3' Rev. 5'-TAGCCGTGAATGGGGGAAAAC-3'
CD206	For. 5'-GTTCACCTGGAGTGATGGTTCTC-3' Rev. 5'-AGGACATGCCAGGGTCACCTTT-3'
CD80	For. 5'-ACAACAGCCTTACCTTCGGG-3' Rev. 5'-TTTGCAGAGCCAGGGTAGTG-3'
NCR1	For. 5'-CTGTGCCTTGGGCTATGTCT-3' Rev. 5'-CCCCCTGACACCAGATGTTC-3'
MART-1	For. 5'-CTTATCGGCTGCTGGTACTG-3' Rev. 5'-CTCTTGAGAAGACAGTCGGC-3'

strategy for lymphoid and myeloid populations is shown in Supplementary Figures S1 and S2.

Statistical analysis. All statistical analyses were performed using GraphPad Prism Version 6 for Windows. Statistical significance between groups was calculated using Student's t-test, except for the *in vitro* experiment, which was calculated using two-way ANOVA. All correlation analyses were calculated by Spearman's rank correlation. Differences between groups were considered significant when the p-value was <0.05. Data in graphs are expressed as mean ± SEM.

Results

Tumor weights. Topical administration of Pliaglis anesthetic cream significantly reduced tumor weight compared to the untreated melanoma animals (MEL+ANE vs. MEL, p=0.0418; MEL+ANE+IMM vs. MEL, p=0.0006; MEL+ANE+IMM vs. MEL+VEH, p=0.0013). Similarly, i.p. administration of the anti-PD-1 antibody resulted in a significant reduction in tumor weight compared to the untreated melanoma animals, and importantly, this effect of anti-PD-1 antibody was potentiated by topical application of anesthetic cream (MEL+IMM vs. MEL, p=0.0177; MEL+ANE+IMM vs. MEL+ANE, p=0.0026) (Figure 2; Table 2).

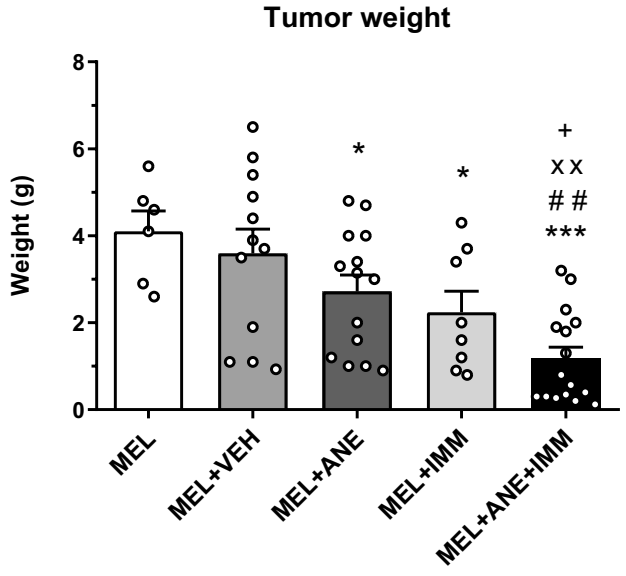

Figure 2. Weight of tumors. Values are expressed as the mean ± SEM. MEL – melanoma without treatment (n=6), MEL+VEH – melanoma+vehicle (n=12), MEL+ANE – melanoma+local anesthetics (n=14), MEL+IMM – melanoma+immunotherapy (n=8), MEL+ANE+IMM – melanoma+local anesthetics+immunotherapy (n=16). Statistical significance between MEL and MEL+VEH, MEL and MEL+ANE, MEL and MEL+IMM, MEL and MEL+ANE+IMM groups: $^{*}p<0.05$; $^{***}p<0.001$. Statistical significance between MEL+VEH and MEL+ANE, MEL+VEH and MEL+IMM, MEL+VEH and MEL+ANE+IMM groups: $^{\#\#}p<0.01$. Statistical significance between MEL+ANE and MEL+IMM, MEL+ANE and MEL+ANE+IMM groups: $^{xx}p<0.01$. Statistical significance between MEL+IMM and MEL+ANE+IMM groups: $^{+}p<0.05$.

Lidocaine and tetracaine exert a synergic cytotoxic effect on murine and human melanoma cells. To evaluate a possible direct effect of Pliaglis on B16F0 melanoma cells observed in an *in vivo* experiment, we exposed melanoma cells to increasing doses of lidocaine (0.5, 1.5, 3 mM) or tetracaine (0.05, 0.1, 0.15 mM) for 72 h. Tetracaine, even at significantly lower concentrations, had potent cytotoxic activity compared to lidocaine (Figure 3A). In addition, to test the potential synergistic effect of lidocaine and tetracaine, we treated melanoma cells with increased concentrations of the combination of lidocaine and tetracaine. The concentrations have been used in the following combinations: 0.5 mM lidocaine + 0.05 mM tetracaine, 1.5 mM lidocaine + 0.1 mM tetracaine or 3 mM lidocaine + 0.15 mM tetracaine. Interestingly, we observed a synergistic cytotoxic effect of these two drugs even at the lowest concentrations where these drugs individually had only a modest effect (Figure 3A). In addition, we also tested the effect of the anesthetics used on the human melanoma cell line A375. We found a similar effect of the used tetracaine and lidocaine on the human melanoma cell (Figure 3B).

Gene expression of p53, PD-L1, pro- and anti-inflammatory factors, IFN-γ, perforin 1, and neurotransmitter receptors in tumor tissue. To investigate the mechanisms responsible for the observed effects of anesthetics, we determined the melanoma gene expression of p53, programmed cell death ligand-1 protein, pro- and anti-inflammatory factors, IFN-γ, perforin 1, and neurotransmitter receptors.

We found significantly reduced gene expression of p53 in the MEL+ANE+IMM group compared to the MEL (p=0.0066), MEL+VEH (p=0.0495), MEL+ANE (p=0.0206) and MEL+IMM (p=0.0403) groups (Figure 4A). In animals treated with therapeutic anti-PD-1 antibody (MEL+IMM and MEL+ANE+IMM groups), we observed significantly increased expression of PD-L1 compared to the MEL group (MEL+IMM vs. MEL, p=0.0030; MEL+ANE+IMM vs. MEL, p=0.0090). Similarly, anti-PD-1 antibody treatment resulted in significantly increased PD-L1 gene expression compared to the MEL+VEH group (MEL+IMM vs. MEL+VEH, p=0.0037; MEL+ANE+IMM vs. MEL+VEH, p=0.0122). Additionally, PD-L1 gene expression was significantly increased in immunotherapy-treated animals compared to Pliaglis alone treated animals (MEL+IMM vs. MEL+ANE, p=0.0156) (Figure 4B). Therapeutic application of anti-PD-1 antibody and Pliaglis significantly increased COX2 expression in tumor tissues in the MEL+ANE, MEL+IMM, and MEL+ANE+IMM groups compared to the MEL group (MEL+ANE vs. MEL, p=0.0302; MEL+IMM vs. MEL, p=0.0005; MEL+ANE+IMM vs. MEL, p=0.0004). COX2 expression was also significantly increased in MEL+IMM and MEL+ANE+IMM tumor tissues compared to the MEL+VEH group (MEL+IMM vs. MEL+VEH, p=0.0014; MEL+ANE+IMM vs. MEL+VEH, p=0.0009). Additionally, COX2 expression was significantly increased by the anti-PD-1 antibody and Pliaglis application compared to

Table 2. Values of tumor weight, gene expression of cancer and immune related factors, neurotransmitter receptors and nerve growth factors, and percentage of immune cells in melanoma tissues.

	MEL (mean±SEM)	MEL+VEH (mean±SEM)	MEL+ANE (mean±SEM)	MEL+IMM (mean±SEM)	MEL+IMM+ANE (mean±SEM)
Tumor weight (g)	4.10±0.47	3.59±0.56	2.72±0.38*	2.24±0.48*	1.18±0.26$^{+,xx,\#\#,***}$
COX2 (relative expression)	1.00±0.50	2.74±2.17	7.05±5.77*	9.93±1.49$^{\#\#,***}$	15.44±5.69$^{x,\#\#\#,***}$
IL1-1β (relative expression)	1.00±0.46	2.25±0.59	3.23±0.77	3.11±0.70	5.83±1.62$^{\#,**}$
IL-6 (relative expression)	1.00±0.28	1.26±0.72	1.45±0.24	1.50±0.19	2.28±0.34$^{\#,*}$
IL-10 (relative expression)	1.00±0.59	3.85±1.27	1.33±1.42	12.32±2.37$^{xx,\#\#,**}$	14.33±3.92$^{xx,\#,**}$
NGF (relative expression)	1.00±0.16	1.19±0.18	1.66±0.20*	1.86±0.26$^{\#,*}$	1.25±0.25
PD-L1 (relative expression)	1.00±0.29	1.32±0.48	1.69±0.55	3.05±0.41$^{x,\#\#,**}$	2.89±0.96$^{\#,**}$
TNF-α (relative expression)	1.00±0.41	1.86±0.55	0.87±0.89	5.70±1.15$^{xx,\#,**}$	6.52±1.90$^{xx,\#,*}$
ADRB2 (relative expression)	1.00±0.12	1.67±0.25*	1.57±0.52	3.02±0.55$^{xx,\#\#,***}$	3.15±0.65$^{x,\#,**}$
FOXP3 (relative expression)	1.00±0.74	1.65±0.55	1.57±0.84	4.60±0.93$^{x,\#,**}$	3.66±1.61$^{x,\#,**}$
IFN-γ (relative expression)	1.00±1.12	3.97±2.27	3.27±3.19	30.81±7.45$^{xx,\#\#,**}$	27.25±6.69$^{xx,\#\#,**}$
p53 (relative expression)	1.00±0.14	0.97±0.08	1.01±0.08	0.97±0.09	0.79±0.04$^{+,x,\#,**}$
Ly-6G (relative expression)	1.00±0.28	2.21±0.86	2.45±1.61	12.21±2.35$^{xx,\#\#,**}$	13.94±3.46$^{xx,\#\#,**}$
Ly-6C (relative expression)	1.00±0.22	1.48±0.49	1.06±0.78	6.05±1.16$^{xx,\#\#,**}$	5.49±1.44$^{x,\#,**}$
F4/80 (relative expression)	1.00±0.37	2.95±0.90	3.71±1.21	4.09±0.64^{x,**}	7.39±2.10$^{x,\#,*}$
CCL2 (relative expression)	1.00±0.22	0.92±0.16	1.20±0.23	2.44±0.29$^{xx,\#\#\#,***}$	2.03±0.35$^{\#\#,*}$
Perforin 1 (relative expression)	1.00±1.29	1.96±2.00	2.89±1.98	35.01±7.21$^{xx,\#\#,**}$	31.56±9.52$^{x,\#,**}$
TGF-β (relative expression)	1.00±0.13	0.91±0.10	0.91±0.09	1.18±0.10	1.07±0.10
α9nAchR (relative expression)	1.00±0.12	2.85±0.44***	6.48±0.73$^{\#\#\#,****}$	3.61±0.38^{xx,***}	7.42±1.23$^{++,\#\#,****}$
CD80 (relative expression)	1.00±0.36	2.92±0.51*	4.49±0.84***	1.82±0.52^{x}	5.21±1.14$^{+,**}$
NCR1 (relative expression)	1.00±0.34	4.90±1.72	3.76±3.38	12.02±2.51$^{x,\#,**}$	21.30±5.96$^{x,\#,**}$
p75NTR (relative expression)	1.00±0.19	1.30±0.22	0.74±0.23$^{\#}$	0.32±0.07$^{x,\#\#,**}$	0.25±0.04$^{x,\#\#\#,**}$
VPAC1 (relative expression)	1.00±0.49	2.32±0.38	2.56±0.52	4.52±1.11*	2.68±0.64
MART-1 (relative expression)	1.00±0.06	1.42±0.19	1.25±0.12	1.14±0.10	1.00±0.09
5-HT2a (relative expression)	1.00±0.35	1.67±0.86	5.18±1.48$^{\#,**}$	2.09±0.47^{x}	4.64±2.01$^{+,\#\#,***}$
CCL11 (relative expression)	1.00±0.37	3.21±0.92	6.26±2.33	4.51±0.50$^{xx,\#,***}$	11.17±3.33$^{x,\#,**}$
CD206 (relative expression)	1.00±0.34	2.03±0.40	2.86±0.65*	1.87±0.34	4.55±0.95$^{+,\#,**}$
CD8^{+} (percentage of cells)	39.02±1.37	42.49±3.95	36.36±2.48	58.31±3.34$^{xxx,\#\#,***}$	51.11±3.56^{xx,**}
CD8-Gr1 (percentage of cells)	33.68±3.37	29.22±2.82	37.06±3.45	23.00±2.22^{xx,*}	26.92±1.71^{x}
MDSC (percentage of cells)	26.07±4.71	16.75±1.93	23.73±1.63$^{\#}$	21.05±1.67	26.35±1.38$^{+,\#\#\#}$
CD11b^{+}Gr1$_{int}$ (percentage of cells)	8.79±0.80	7.07±0.72	9.47±0.55$^{\#}$	10.99±0.88$^{\#\#}$	12.29±0.67$^{xx,\#\#\#\#,**}$
CD11b^{+}Gr1$_{high}$ (percentage of cells)	17.28±4.16	9.68±1.29*	14.26±1.15$^{\#}$	10.06±0.86^{xx}	14.06±0.91$^{++,\#}$
CD11^{+}Gr1^{-} (percentage of cells)	63.53±3.67	71.77±1.59*	66.54±1.20$^{\#}$	71.35±1.57^{x}	65.68±1.25$^{+,\#\#}$

Notes: MEL group - animals with intradermally injected melanoma cells (n=6); MEL+VEH group - animals with intradermally injected melanoma cells and topically administered vehicle ointment on the surface of the melanoma (n=12); MEL+ANE - animals with intradermally injected melanoma cells and topically administered Pliaglis anesthetic cream on the surface of the melanoma (n=14); MEL+IMM - animals with intradermally injected melanoma cells and intraperitoneally administered anti PD-1 antibody (n=8); MEL+ANE+IMM - animals with intradermally injected melanoma cells and combined treatment with Pliaglis and anti PD-1 antibody (n=16). Values are expressed as mean ± standard error of the mean (SEM). Statistical significance between MEL and MEL+VEH, MEL and MEL+ANE, MEL and MEL+IMM, MEL and MEL+ANE+IMM groups: *p<0.05; **p<0.01, ***p<0.001, ****p<0.0001. Statistical significance between MEL+VEH and MEL+ANE, MEL+VEH and MEL+IMM, MEL+VEH and MEL+ANE+IMM groups: $^{\#}$p<0.05, $^{\#\#}$p<0.01, $^{\#\#\#}$p<0.001, $^{\#\#\#\#}$p<0.0001. Statistical significance between MEL+ANE and MEL+IMM, MEL+ANE and MEL+ANE+IMM groups: ^{x}p<0.05, ^{xx}p<0.01, ^{xxx}p<0.001. Statistical significance between MEL+IMM and MEL+ANE+IMM groups: $^{+}$p<0.05, $^{++}$p<0.01.

the MEL+ANE group (MEL+ANE+IMM vs. MEL+ANE, p=0.0328) (Figure 4C). Furthermore, we found that COX2 expression was negatively correlated with tumor weight in the MEL+ANE and MEL+ANE+IMM groups (MEL+ANE, r=–0.5859, p=0.0295; MEL+ANE+IMM, r=–0.6044, p=0.0248). The combined treatment significantly increased the expression of IL-1β compared to the MEL (p=0.0069) and MEL+VEH (p=0.0265), but no statistical differences were shown compared to the other groups (Figure 4D). Similarly, the combined treatment increased the expression of IL-6 compared to the MEL (p=0.0220) and MEL+VEH (p=0.0161) groups, and the MEL+ANE and MEL+IMM groups were considerably changed compared to the MEL+ANE+IMM group (MEL+ANE, p=0.0596; MEL+IMM, p=0.0592) (Figure 4E). Expression of IL-6 in the MEL+ANE+IMM group was negatively correlated with tumor weight (r=–0.7504, p=0.0011). The anti-PD-1 antibody-treated groups had significantly increased expression of TNF-α compared to the MEL group (MEL+IMM vs. MEL, p=0.0061; MEL+ANE+IMM vs. MEL, p=0.0162).

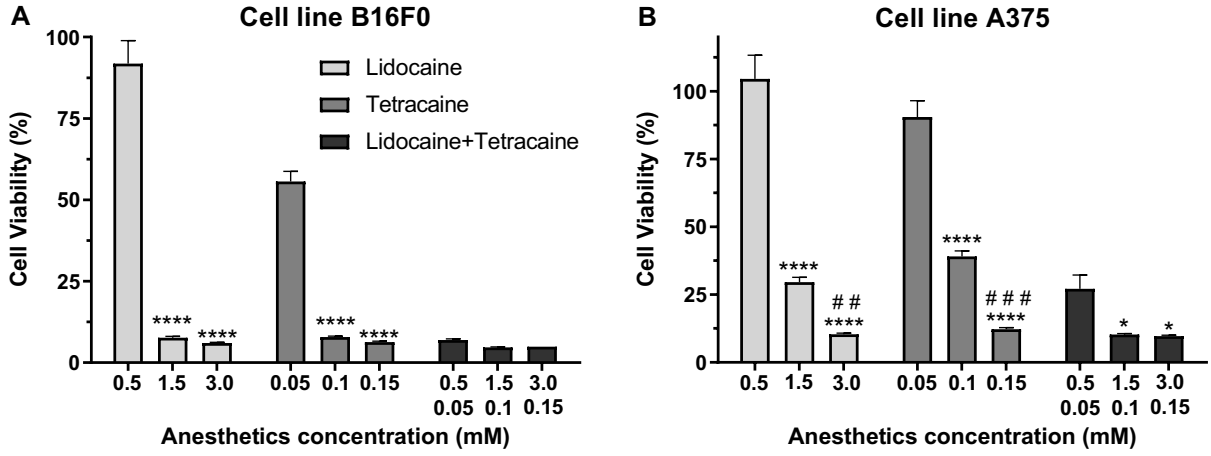

Figure 3. A direct effect of anesthetic on B16F0 (A) and A375 (B) cell viability. Melanoma cell lines were incubated for 72 h with lidocaine, tetracaine, or a combination of lidocaine and tetracaine in different concentrations. Cell viability was calculated as the percentage of viable cancer cells exposed to anesthetics compared to the control cancer cells. Values are expressed as the mean ± SEM. Statistical significance between 0.5 and 1.5 mM, 0.5 and 3.0 mM, 0.05 and 0.1 mM, 0.05 and 0.15 mM concentrations: ****p<0.0001. Statistical significance between 1.5 and 3.0 mM, 0.1 and 0.15 mM concentrations: ##p<0.01, ###p<0.001.

The same results were observed when compared to the MEL+VEH group (MEL+IMM vs. MEL+VEH, p=0.0126; MEL+ANE+IMM vs. MEL+VEH, p=0.0302). Furthermore, TNF-α expression was significantly higher in MEL+IMM and MEL+ANE+IMM compared to the MEL+ANE group (MEL+IMM vs. MEL+ANE, p=0.0038; MEL+ANE+IMM vs. MEL+ANE, p=0.0095) (Figure 4F). We found that the gene expression of IL-10 was significantly increased by the anti-PD-1 antibody compared to MEL (MEL+IMM vs. MEL, p=0.0024; MEL+ANE+IMM vs. MEL, p=0.0052). Similarly, increased gene expression of IL-10 was observed in these tumors compared to the MEL+VEH group (MEL+IMM vs. MEL+VEH, p=0.0096; MEL+ANE+IMM vs. MEL+VEH, p=0.0201). Significant changes in IL-10 were also observed compared to animals treated with Pliaglis alone (MEL+IMM vs. MEL+ANE, p=0.0024; MEL+ANE+IMM vs. MEL+ANE, p=0.0046) (Figure 4G; Table 2). The gene expression of IL-10 in the MEL+ANE+IMM group was negatively correlated with tumor weight in contrast to the MEL+IMM group (MEL+ANE+IMM, r=–0.7349, p=0.0016; MEL+IMM, r=–0.1905, p=0.6646). We found no effect of anesthetics or immunotherapy on TGF-β gene expression (Figure 4H).

We observed a significant increase in gene expression of INF-γ in both MEL+IMM and MEL+ANE+IMM groups compared to untreated animals (MEL+IMM vs. MEL, p=0.0061; MEL+IMM vs. MEL+VEH, p=0.0084; MEL+ANE+IMM vs. MEL, p=0.0021; MEL+ANE+IMM vs. MEL+VEH, p=0.0038). Compared to animals treated with local anesthetic alone, IFN-γ expression was significantly higher in the MEL+IMM and MEL+ANE+IMM groups (MEL+IMM vs. MEL+ANE, p=0.0075; MEL+ANE+IMM vs. MEL+ANE, p=0.0030) (Figure 4I). We also observed a similar response in perforin 1 gene expression in tumor tissues obtained from these animals (MEL+IMM vs. MEL, p=0.0025; MEL+IMM vs. MEL+VEH, p=0.0035; MEL+IMM vs. MEL+ANE, p=0.0034; MEL+ANE+IMM vs. MEL, p=0.0080; MEL+ANE+IMM vs. MEL+VEH, p=0.0131; MEL+ANE+IMM vs. MEL+ANE, p=0.0129) (Figure 4J). Interestingly, the gene expression of the α9 nicotinic receptor subunit (α9nAChR) was significantly increased by vehicle ointment compared to the MEL group (MEL+VEH vs. MEL, p=0.0017). The local anesthetic application also resulted in a significant increase in α9nAChR compared to the MEL and MEL+VEH groups (MEL+ANE vs. MEL, p<0.0001; MEL+ANE vs. MEL+VEH, p=0.0004; MEL+ANE+IMM vs. MEL, p<0.0001; MEL+ANE+IMM vs. MEL+VEH). Treatment with anti-PD-1 antibody resulted in a significant increase in α9nAChR (MEL+IMM vs. MEL, p=0.0002; MEL+IMM vs. MEL+ANE, p=0.0025; p=0.0023). Finally, a significant increase in α9nAChR expression was also observed when comparing MEL+ANE+IMM and immunotherapy-only animals (MEL+ANE+IMM vs. MEL+IMM, p=0.0079) (Figure 4K; Table 2). Furthermore, we observed a significant local anesthetic-induced increase in serotonin receptor 5-HT2a gene expression compared to the untreated animals and animals treated with immunotherapy alone (MEL+ANE vs. MEL, p=0.0039; MEL+ANE vs. MEL+VEH, p=0.0124; MEL+IMM vs. MEL+ANE, p=0.0479; MEL+ANE+IMM vs. MEL, p=0.0005; MEL+ANE+IMM vs. MEL+VEH, p=0.0015; MEL+ANE+IMM vs. MEL+IMM, p=0.0079) (Figure 4L; Table 2).

Gene expression of selected cancer-related immune factors. To elucidate the pathways mediating the anticancer effect of the anesthetic in melanoma bearing mice, we also

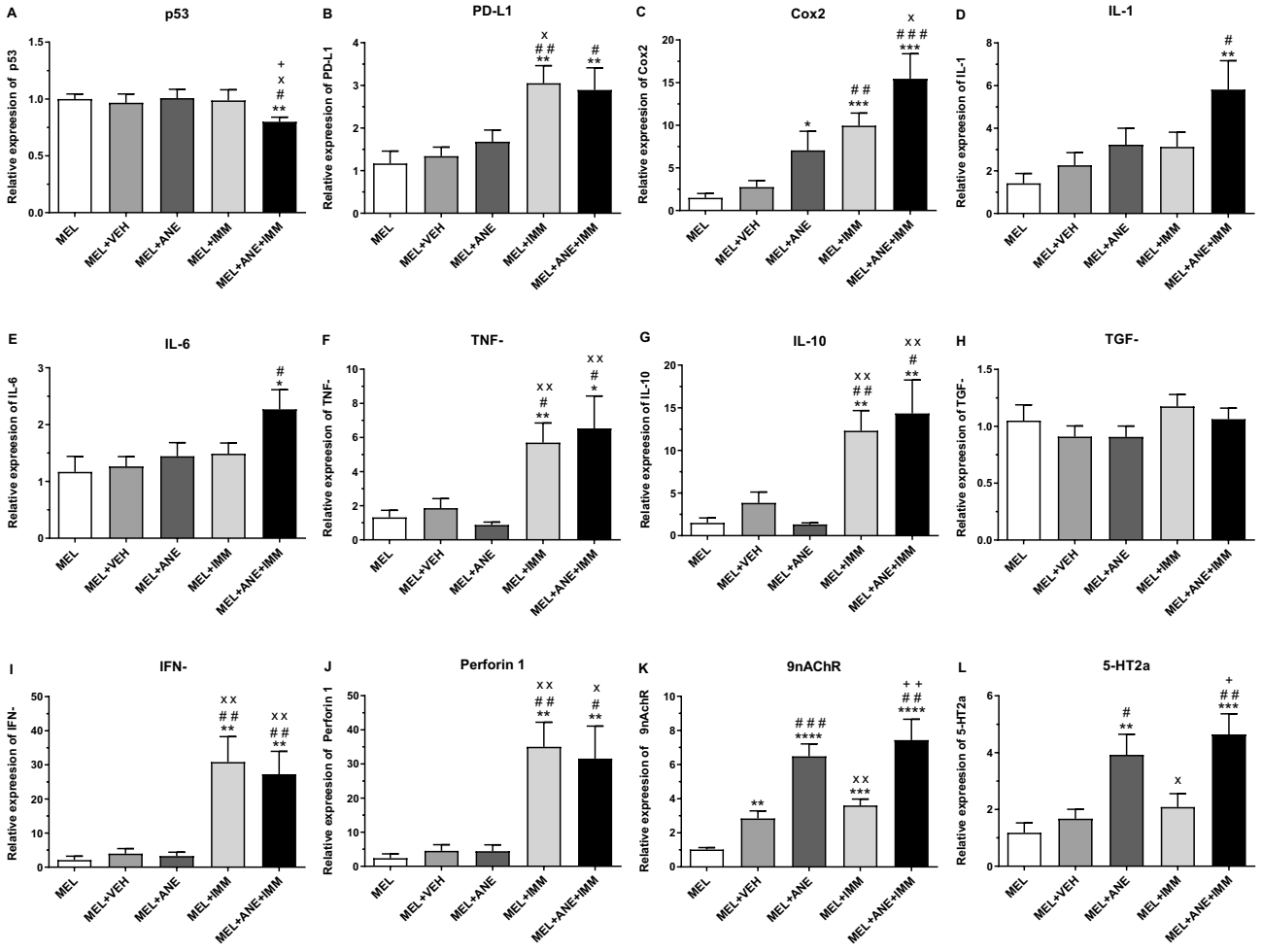

Figure 4. Gene expression of p53 (A), PD-L1 (B), cyclooxygenase 2 (COX2) (C), interleukin IL-1β (IL-1β) (D), interleukin 6 (IL-6) (E), tumor necrosis factor α (TNF-α) (F), interleukin 10 (IL-10) (G), transforming growth factor β (TGF-β) (H), interferon γ (IFN-γ) (I), perforin 1 (J), nicotinic acetylcholine receptor α9 subunit (α9nAChR) (K), 5-HT2a (L). Data are presented as a fold change relative to control, taken as 1. Values are expressed as the mean ± SEM. MEL – melanoma without treatment (n=6), MEL+VEH – melanoma+vehicle (n=12), MEL+ANE – melanoma+local anesthetics (n=14), MEL+IMM – melanoma+immunotherapy (n=8), MEL+ANE+IMM – melanoma+local anesthetics+immunotherapy (n=16). Statistical significance between MEL and MEL+VEH, MEL and MEL+ANE, MEL and MEL+IMM, MEL and MEL+ANE+IMM groups: $^{*}p<0.05$; $^{**}p<0.01$, $^{***}p<0.001$, $^{****}p<0.0001$. Statistical significance between MEL+VEH and MEL+ANE, MEL+VEH and MEL+IMM, MEL+VEH and MEL+ANE+IMM groups: $^{\#}p<0.05$, $^{\#\#}p<0.01$, $^{\#\#\#}p<0.001$. Statistical significance between MEL+ANE and MEL+IMM, MEL+ANE and MEL+ANE+IMM groups: $^{x}p<0.05$, $^{xx}p<0.01$. Statistical significance between MEL+IMM and MEL+ANE+IMM groups: $^{+}p<0.05$, $^{++}p<0.01$.

determined the gene expression of selected factors known to be involved in the immune system response to cancer (melanoma).

We found significantly increased expression of FOXP3 in mice exposed to immunotherapy compared to the MEL and MEL+VEH groups (MEL+IMM vs. MEL, p=0.0063; MEL+ANE+IMM vs. MEL, p=0.0085; MEL+IMM vs. MEL+VEH, p=0.0063; MEL+ANE+IMM vs. MEL+VEH, p=0.0085). Moreover, immunotherapy also increased FOXP3 expression compared to the MEL+ANE group (MEL+IMM vs. MEL+ANE, p=0.0139; MEL+ANE+IMM vs. MEL+ANE, p=0.0350) (Figure 5A; Table 2). Gene expression of FOXP3 was negatively correlated with tumor weight in the MEL+ANE+IMM group, but not in the MEL+IMM group (MEL+ANE+IMM, r=–0.7152, p=0.0024; MEL+IMM, r=–0.2874, p=0.4714). A significant increase in Ly-6C and Ly-6G was observed in the MEL+IMM and MEL+ANE+IMM groups compared to the MEL group (Ly-6C: MEL+IMM vs. MEL, p=0.0037; MEL+ANE+IMM vs. MEL, p=0.0086; Ly-6G: MEL+IMM vs. MEL, p=0.0021; MEL+ANE+IMM vs. MEL, p=0.0022). This significant change was also observed compared to the MEL+VEH and MEL+ANE groups (Ly-6C: MEL+IMM vs. MEL+VEH, p=0.0053; MEL+ANE+IMM vs. MEL+VEH, p=0.0148; MEL+IMM

vs. MEL+ANE, p=0.0046; MEL+ANE+IMM vs. MEL+ANE, p=0.0137; Ly-6G: MEL+IMM vs. MEL+VEH, p=0.0035; MEL+ANE+IMM vs. MEL+VEH, p=0.0041; MEL+IMM vs. MEL+ANE, p=0.0039; MEL+ANE+IMM vs. MEL+ANE, p=0.0086) (Figures 5B, 5C). Ly6C and Ly6G gene expression was negatively correlated with tumor weight in both groups (MEL+ANE+IMM Ly-6G, r=–0.7211, p=0.0022; MEL+IMM Ly-6G, r=–0.8571, p=0.0107 and MEL+ANE+IMM Ly-6C, r=–0.6583, p=0.0063). Furthermore, we found that in our experimental model, Ly-6C and Ly-6G expres-

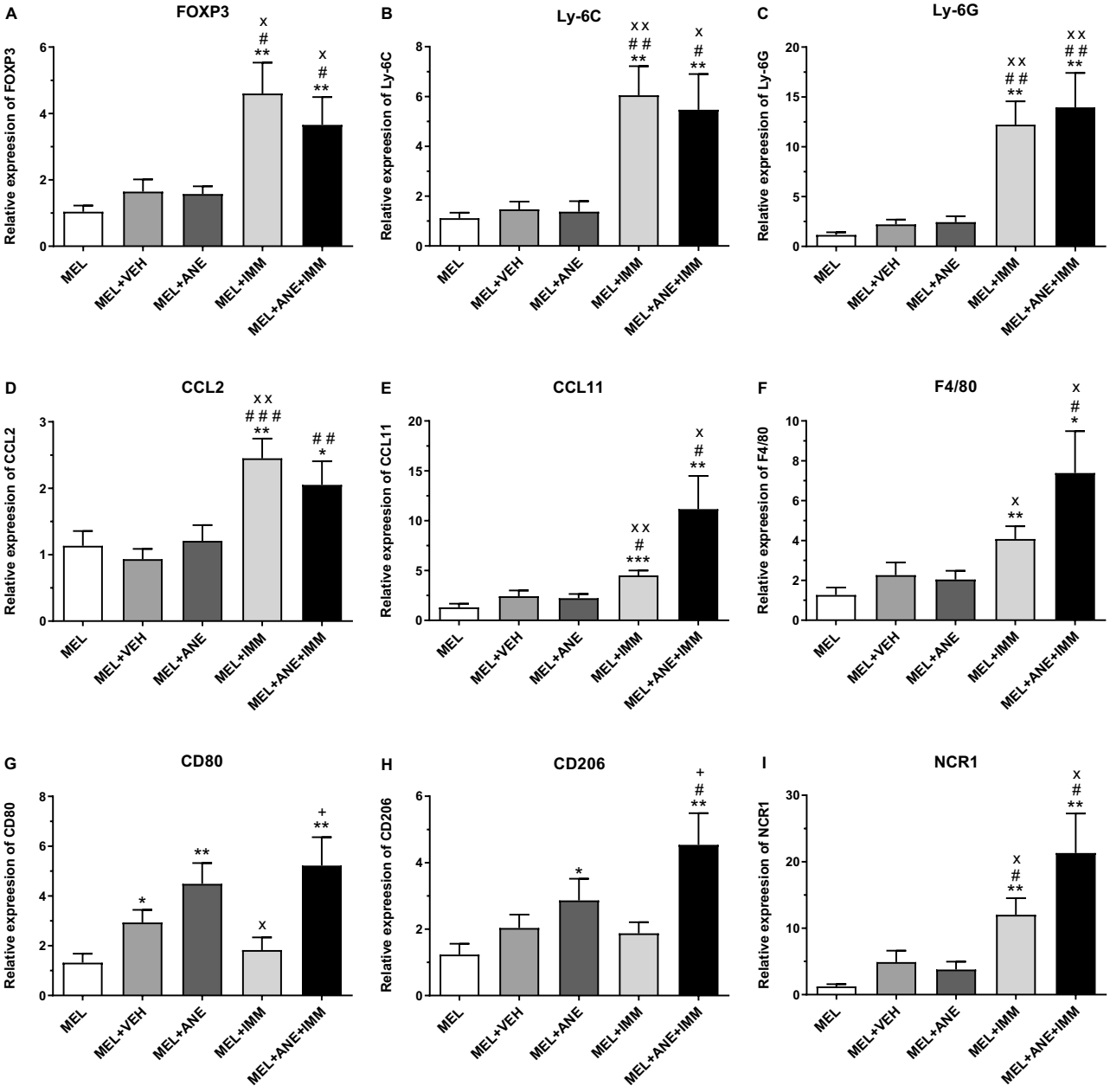

Figure 5. Gene expression of FOXP3 (A), Ly-6C (B), Ly-6G (C), CCL2 (D), CCL11 (E), F4/80 (F), CD80 (G), CD206 (H), and NCR1 (I). Data are presented as a fold change relative to control, taken as 1. Values are expressed as the mean ± SEM. MEL – melanoma without treatment (n=6), MEL+VEH – melanoma+vehicle (n=12), MEL+ANES – melanoma+local anesthetics (n=14), MEL+IMMUNO – melanoma+immunotherapy (n=8), MEL+ANES+IMMUNO – melanoma+local anesthetics+immunotherapy (n=16). Statistical significance between MEL and MEL+VEH, MEL and MEL+ANE, MEL and MEL+IMM, MEL and MEL+ANE+IMM groups: $^{*}p<0.05$; $^{**}p<0.01$, $^{***}p<0.001$. Statistical significance between MEL+VEH and MEL+ANE, MEL+VEH and MEL+IMM, MEL+VEH and MEL+ANE+IMM groups: $^{\#}p<0.05$, $^{\#\#}p<0.01$, $^{\#\#\#}p<0.001$. Statistical significance between MEL+ANE and MEL+IMM, MEL+ANE and MEL+ANE+IMM groups: $^{x}p<0.05$, $^{xx}p<0.01$. Statistical significance between MEL+IMM and MEL+ANE+IMM groups: $^{+}p<0.05$.

sion is highly positively correlated with CCL2 expression (MEL+ANE+IMM Ly-6C, r=0.8966, p≤0.0001; Ly-6G, r=0.8895, p≤0.0001; MEL+IMM Ly-6C, r=0.7785, p=0.0295; Ly-6G, r=0.7545, p=0.0377). We also observed an increase in CCL2 and CCL11 immunotherapy-treated melanomas compared to the MEL, MEL+VEH and MEL+ANE groups (CCL2: MEL+IMM vs. MEL, p=0.0041; MEL+ANE+IMM vs. MEL, p=0.0413; MEL+IMM vs. MEL+VEH, p=0.0009; MEL+ANE+IMM vs. MEL+VEH, p=0.0092; MEL+IMM vs. MEL+ANE, p=0.0050; CCL11: MEL+IMM vs. MEL, p=0.0002; MEL+ANE+IMM vs. MEL, p=0.0099; MEL+IMM vs. MEL+VEH, p=0.0130; MEL+ANE+IMM vs. MEL+VEH, p=0.0201; MEL+IMM vs. MEL+ANE, p=0.0031; MEL+ANE+IMM vs. MEL+ANE, p=0.0174) (Figures 5D, 5E). Immunotherapy significantly improved F4/80 expression in melanomas compared to the MEL, MEL+VEH and MEL+ANE groups (MEL+IMM vs. MEL, p=0.0032; MEL+ANE+IMM vs. MEL, p=0.0111; MEL+ANE+IMM vs. MEL+VEH, p=0.0315; MEL+IMM vs. MEL+ANE, p=0.0216; MEL+ANE+IMM vs. MEL+ANE, p=0.0238) (Figure 5F; Table 2). Gene expression of F4/80 was negatively correlated with tumor weight in the MEL+ANE+IMM group, but not in the MEL+IMM group (MEL+ANE+IMM, r=−0.8150, p=0.0002; MEL+IMM, r=−0.5629, p=0.1435). Furthermore, we found that F4/80 gene expression was significantly correlated with TNF-α expression in the combined therapy-treated group in contrast to the anti-PD-1 antibody alone treated group (MEL+ANE+IMM, r=0.9219, p≤0.0001; MEL+IMM, r=0.5868, p=0.1353). Finally, we found increased NCR1 gene expression after anti-PD-1 treatment compared to the MEL, MEL+VEH and MEL+ANE groups (MEL+IMM vs. MEL, p=0.0035; MEL+ANE+IMM vs. MEL, p=0.0051; MEL+IMM vs. MEL+VEH, p=0.0365; MEL+ANE+IMM vs. MEL+VEH, p=0.0183; MEL+IMM vs. MEL+ANE, p=0.0140; MEL+ANE+IMM vs. MEL+ANE, p=0.0120) (Figure 5I). While anesthetic application did not affect the stimulatory effect of immunotherapy on gene expression of FOXP3, Ly6C, Ly6G, or CCL2, it exaggerated gene expression of CCL11 and NCR1. Compared with the MEL group, anesthetic alone or in combination with immunotherapy exaggerated the gene expression of CD80 and CD206 (CD80: MEL+ANE vs. MEL, p=0.0029; MEL+ANE+IMM vs. MEL, p=0.0044; CD206: MEL+ANE vs. MEL, p=0.0386; MEL+ANE+IMM vs. MEL, p=0.0041) (Figures 5G, 5H). In addition, CD80 expression was negatively correlated with tumor weight only in the MEL+ANE+IMM group in contrast to the MEL+IMM group (MEL+ANE+IMM, r=−0.6328, p=0.0098; MEL+IMM, r=−0.2928, p=0.4565). We suggest that macrophage marker F4/80 was negatively correlated with tumor weight in the MEL+ANE+IMM group due to significantly increased expression of the co-stimulatory molecule CD80 (Figure 5G; Table 2). This molecule is known for its role in T cell activation and is expressed on activated antitumorigenic M1 macrophages [8, 9]. The last immune-associated gene that we identified was the NK cell marker NCR1. In this group, expression was negatively correlated with tumor weight in contrast to the MEL+IMM group (MEL+ANE+IMM, r=−0.7291, p=0.0040; MEL+IMM, r=−0.4286, p=0.2992).

Quantification of selected cell populations in tumor tissue. Groups treated with the anti-PD-1 antibody had a significantly elevated percentage ratio of cytotoxic $CD8^+$ T lymphocytes compared to the MEL and MEL+VEH groups (MEL+IMM vs. MEL, p=0.0004; MEL+IMM vs. MEL+VEH, p=0.0071; MEL+ANE+IMM vs. MEL, p=0.0052). In addition, the percentage of $CD8^+$ T cells was increased by anti-PD-1 antibody treatment compared to the MEL+ANE (MEL+IMM vs. MEL+ANE, p=0.0001; MEL+ANE+IMM vs. MEL+ANE, p=0.0022) (Figure 6A). We then investigated the $CD8^+Gr1$ cells, because it has been shown that Gr1 is expressed on memory $CD8^+CD44_{high}CD62L_{high}$ T cells [10]. Moreover, this marker has been shown to be present on central memory CD8 T cells [11]. We found that anti-PD-1 antibody treatment resulted in a significant decrease in the percentage of $CD8^+Gr1$ cells compared to the MEL and MEL+ANE groups (MEL+IMM vs. MEL, p=0.0173; MEL+IMM vs. MEL+ANE, p=0.0027; MEL+ANE+IMM vs. MEL+ANE, p=0.0162). Finally, local anesthetic moderately increased the percentage of this population compared to the MEL+VEH group (p=0.0916) (Figure 6B; Table 2).

In addition, we examined changes in the myeloid population, specifically in $CD11b^+Gr1^-$ and $CD11b^+Gr1^+$ cells. Daily treatment with local anesthetic elevated the percentage of $CD11b^+Gr1^+$ cells compared to the MEL+VEH and MEL+IMM groups (MEL+ANE vs. MEL+VEH, p=0.0115; MEL+ANE+IMM vs. MEL+VEH, p=0.0007; MEL+ANE+IMM vs. MEL+IMM, p=0.0260) (Figure 6C). Due to deeper analysis, we divided MDSC according to CD11b and Gr1 markers on $CD11b^+Gr1_{int}$, $CD11b^+Gr1_{high}$ according to Rhyzov et al. [12]. Local anesthetic and immunotherapy-treated groups had a moderately elevated percentage of $CD11b^+Gr1_{int}$ cells compared to the MEL and MEL+VEH groups (MEL+ANE vs. MEL+VEH, p=0.0149; MEL+IMM vs. MEL+VEH, p=0.0035; MEL+ANE+IMM vs. MEL, p=0.0057; MEL+ANE+IMM vs. MEL+VEH, p≤0.0001). Additionally, an elevated percentage of $CD11b^+Gr1_{int}$ cells was observed in the MEL+ANE+IMM group compared to the MEL+ANE group (p=0.0030) (Figure 6D). The $CD11b^+Gr-1_{high}$ cell subset percentage was increased in the groups treated with local anesthetics compared to the MEL+VEH (MEL+ANE vs. MEL+VEH, p=0.0148; MEL+ANE+IMM vs. MEL+VEH, p=0.0119). In addition, the percentage of $CD11b^+Gr-1_{high}$ cells was also increased in the MEL+VEH group compared to the MEL group (p=0.0449), and in the MEL+ANE+IMM group compared to the MEL+IMM group (p=0.0044) (Figure 6E). In the anti-PD-1 antibody alone-treated group was moderately increased the percentage ratio of $CD11b^+Gr1^-$ cells compared to the MEL group (p=0.0523). On the other hand, in the groups treated with local anesthetics, the percentage of $CD11b^+Gr1^-$ cells was decreased compared to the MEL+VEH group (MEL+ANE

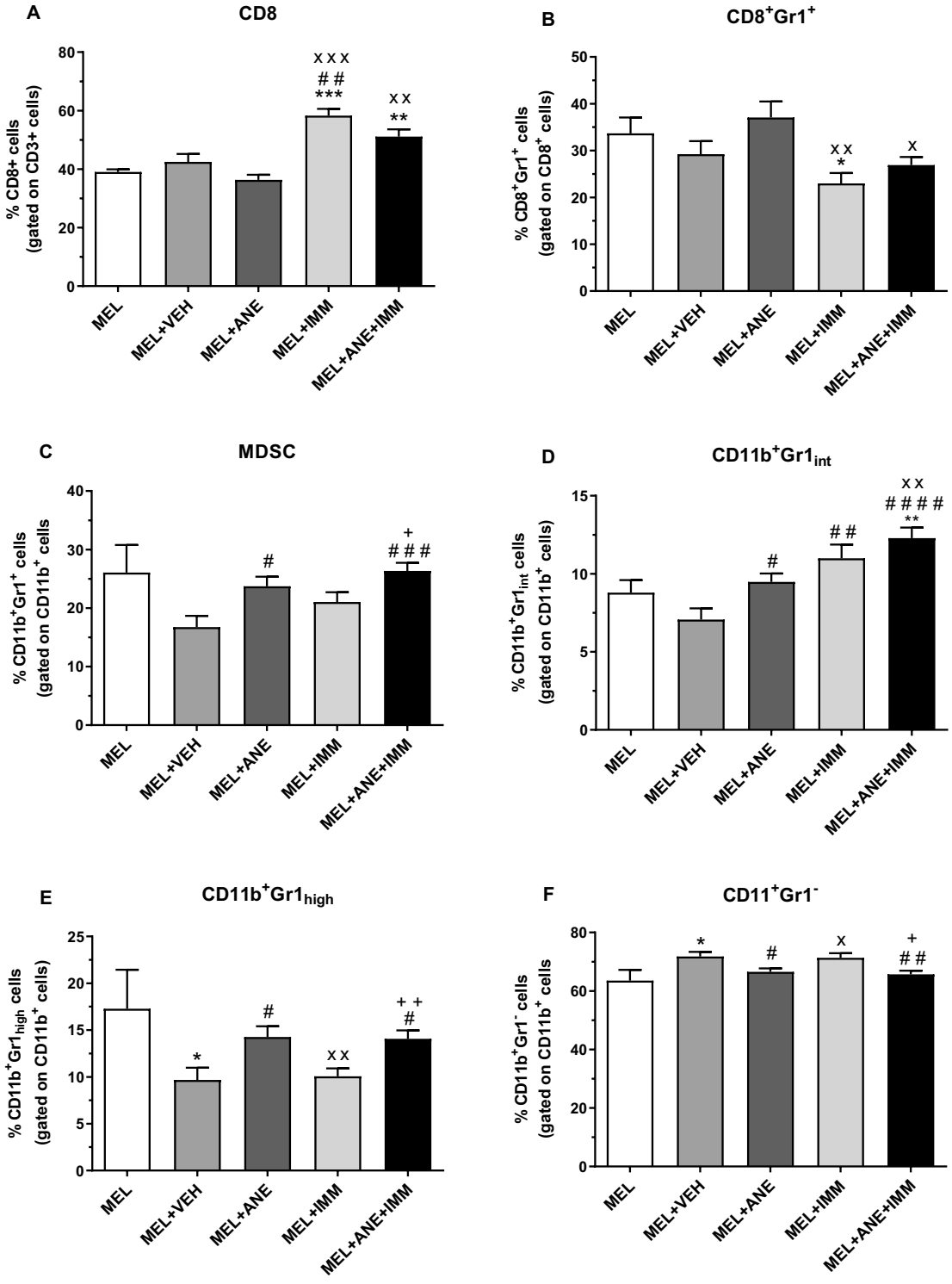

Figure 6. Percentage of CD8 (A), CD8Gr-1 (B), MDSC (C), CD11b$^+$Gr-1$_{int}$ (D), CD11b$^+$Gr-1$_{high}$ (E), and CD11b$^+$Gr-1$^-$ (F) cells measured by flow cytometry. Values are expressed as the mean ± SEM. MEL – melanoma without treatment (n=6), MEL+VEH – melanoma+vehicle (n=12), MEL+ANE – melanoma+local anesthetics (n=14), MEL+IMM – melanoma+immunotherapy (n=8), MEL+ANE+IMM – melanoma+local anesthetics+immunotherapy (n=16). Statistical significance between MEL and MEL+VEH, MEL and MEL+ANE, MEL and MEL+IMM, MEL and MEL+ANE+IMM groups: $^*p<0.05$; $^{**}p<0.01$, $^{***}p<0.001$. Statistical significance between MEL+VEH and MEL+ANE, MEL+VEH and MEL+IMM, MEL+VEH and MEL+ANE+IMM groups: $^{\#}p<0.05$, $^{\#\#}p<0.01$, $^{\#\#\#}p<0.001$, $^{\#\#\#\#}p<0.0001$. Statistical significance between MEL+ANE and MEL+IMM, MEL+ANE and MEL+ANE+IMM groups: $^{x}p<0.05$, $^{xx}p<0.01$. Statistical significance between MEL+IMM and MEL+ANE+IMM groups: $^{+}p<0.05$, $^{++}p<0.01$.

vs. MEL+VEH, p=0.0134; MEL+ANE+IMM vs. MEL+VEH, p=0.0055). Additionally, we found an increased percentage of $CD11b^+Gr1^-$ cells in the MEL+VEH group compared to the MEL group (p=0.0295), increased percentage of these cells in the MEL+IMM group compared to the MEL+ANE group (p=0.0248) and decreased percentage of $CD11b^+Gr1^-$ cells in the MEL+ANE+IMM group compared to the MEL+IMM group (p=0.0127) (Figure 6F; Table 2). We observed a very high negative correlation between $CD11b^+Gr1^+$ cells and $CD11b^+Gr1^-$ (MEL+ANE+IMM, r=–0.9654, p≤0.0001). For a deeper analysis, we correlated $CD11b^+Gr1^-$ cells with the subsets of $CD11b^+Gr1^+$ cells. Cells from the population of $CD11b^+Gr1^-$ was negatively correlated with $CD11b^+Gr1_{int}$, but mainly with the $CD11b^+Gr1_{high}$ population ($CD11b^+Gr1_{int}$, r=–0.7682, p=0.0008; $CD11b^+Gr1_{high}$, r=–0.8799, p≤0.0001).

Gene expression of selected receptors for neurotransmitters in tumor tissue. We have found that the gene expression of β_2-adrenergic receptors was significantly increased in the anti-PD-1 antibody-treated groups and MEL+VEH compared to the MEL group (MEL+VEH, p=0.0398; MEL+IMM vs. MEL, p=0.0008; MEL+ANE+IMM vs. MEL, p=0.0056). Additionally, we observed a significant increase in β_2-adrenergic receptors expression after anti-PD-1 antibody treatment compared to the MEL+VEH and MEL+ANE (MEL+IMM vs. MEL+VEH, p=0.0077; MEL+ANE+IMM vs. MEL+VEH, p=0.0454; MEL+IMM vs. MEL+ANE, p=0.0047; MEL+ANE+IMM vs. MEL+ANE, p=0.0329) (Figure 7A; Table 2). Interestingly, gene expression was negatively correlated with tumor weight only in the groups treated with a local anesthetic (MEL+ANE, r=–0.5530, p=0.0402; MEL+ANE+IMM, r=–0.7422, p=0.0013). In addition, we showed that the neurotransmitter receptors for the vasoactive intestinal peptide VPAC1 and for substance P NK-1R were affected only in the MEL+IMM group (VPAC1: MEL+IMM vs. MEL, p=0.0251; NK-1R: MEL+IMM vs. MEL+VEH, p=0.0129; MEL+IMM+MEL+ANE, p=0.0075). We also observed a significant increase in NK-1R expression in the MEL+ANE+IMM group compared to the

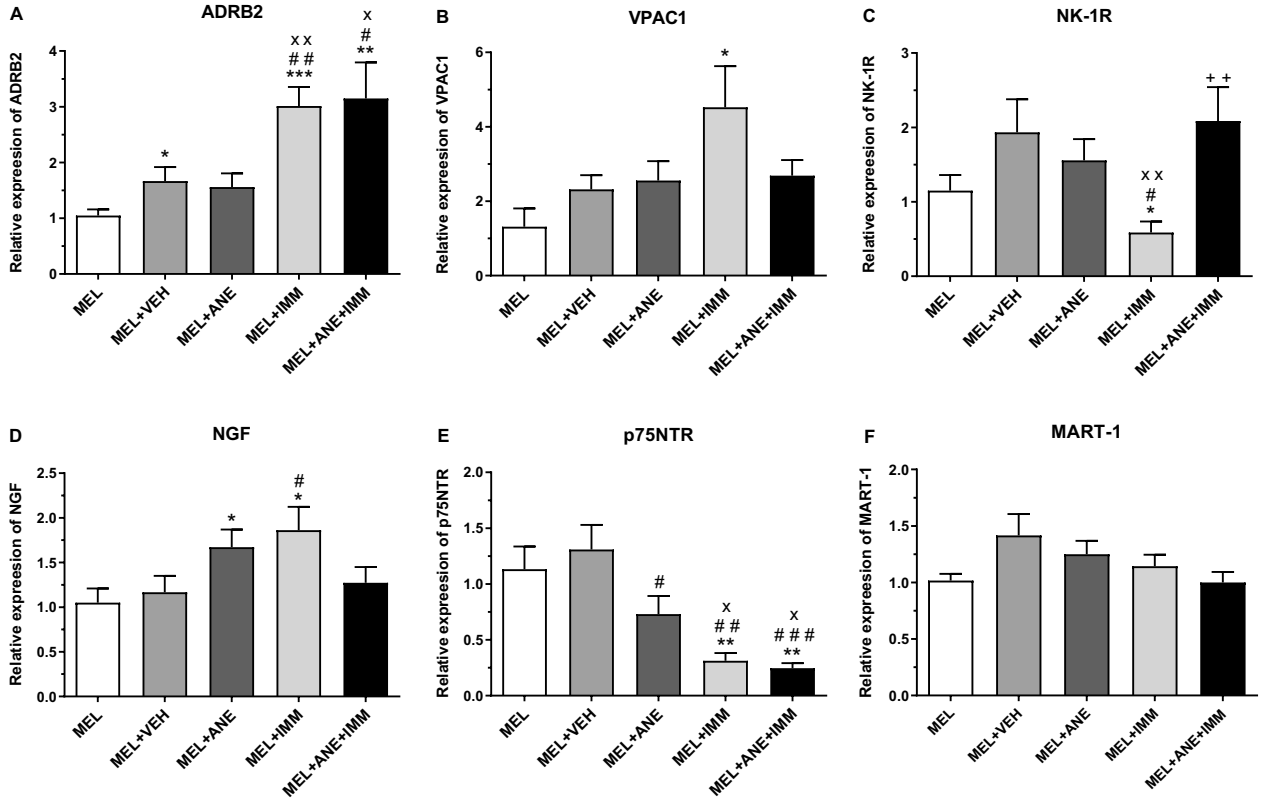

Figure 7. Gene expression of β_2-adrenergic receptor (ADRB2) (A), Vasoactive intestinal polypeptide receptor 1 (VPAC1) (B), Neurokinin-1 Receptor (NK-1R) (C), Nerve growth factor (NGF) (D), p75NTR (E) and Melanoma-associated antigen recognized by T cells 1 (MART-1) (F). Data are presented as fold change relative to control, taken as 1. Values are expressed as the mean ± SEM. MEL – melanoma without treatment (n=6), MEL+VEH – melanoma+vehicle (n=12), MEL+ANE – melanoma+local anesthetics (n=14), MEL+IMM – melanoma+immunotherapy (n=8), MEL+ANE+IMM – melanoma+local anesthetics+immunotherapy (n=16). Statistical significance between MEL and MEL+VEH, MEL and MEL+ANE, MEL and MEL+IMM, MEL and MEL+ANE+IMM groups: *p<0.05; **p<0.01, ***p<0.001. Statistical significance between MEL+VEH and MEL+ANE, MEL+VEH and MEL+IMM, MEL+VEH and MEL+ANE+IMM groups: #p<0.05, ##p<0.01, ###p<0.001. Statistical significance between MEL+ANE and MEL+IMM, MEL+ANE and MEL+ANE+IMM groups: xp<0.05, xxp<0.01. Statistical significance between MEL+IMM and MEL+ANE+IMM groups: ++p<0.01.

MEL+IMM (MEL+ANE+IMM vs. MEL+IMM, p=0.0057) (Figures 7B, 7C). Groups treated only with the anti-PD-1 antibody and local anesthetic had significantly increased NGF expression compared to the MEL and MEL+VEH groups (MEL+ANE vs. MEL, p=0.0255; MEL+IMM vs. MEL, p=0.0222; MEL+IMM vs. MEL+VEH, p=0.0474) (Figure 7D). Interestingly, local anesthetic had the opposite effect on NGF gene expression in the MEL+ANE+IMM group, where NGF expression was decreased compared to the MEL+IMM group (p=0.0689). Gene expression of the p75 neurotrophin NGF receptor (p75NTR) was significantly decreased by local anesthetics and anti-PD-1 antibody compared to the MEL and MEL+VEH groups (MEL+IMM vs. MEL, p=0.0082; MEL+ANE+IMM vs. MEL, p=0.0064; MEL+ANE vs. MEL+VEH, p=0.0472; MEL+IMM vs. MEL+VEH, p=0.0010; MEL+ANE+IMM vs. MEL+VEH, p=0.0006). Interestingly, p75NTR expression was decreased in MEL+IMM and MEL+ANE+IMM compared to the MEL+ANE group (MEL+IMM vs. MEL+ANE, p=0.0302; MEL+ANE+IMM vs. MEL+ANE, p=0.0120) (Figure 7E; Table 2). Based on these findings, we also determined gene expression of the melanoma-associated antigen recognized by T cells-1 (MART-1), but we found no statistically significant differences between groups (Figure 7F; Table 2).

Gene expression in responders. In our experiment, we used an unmodified B16F0 cell line for melanoma induction. This tumor model is almost non-immunogenic and the anti-PD1 therapy produces stable antitumor immunity only in 30% of mice [13]. Similar findings were also observed in patients with melanoma [14]. Therefore, melanoma patients might be divided into "responders" and "non-responders". For our analysis, we simply divided animals into these two groups based on tumor weight. The group with the upper half values of tumor weight we designated as "non-responders" and the group with the lower half as "responders". We used for our analysis only groups treated with anti-PD-1 antibody. In animals from these groups, we compared tumor weights and gene expression of responders between the MEL+ANE+IMM and MEL+IMM groups. The average tumor weight of MEL+IMM responders was 0.90±0.11 g, and the average tumor weight of MEL+ANE+IMM responders was 0.37±0.07 g. The average tumor weight of MEL+IMM non-responders was 3.25±1.16 g, and the average tumor weight of MEL+ANE+IMM non-responders was 2.21±0.26 g.

Tumor weights between these two groups were significantly higher in the MEL+IMM group in responders (MEL+ANE+IMM vs. MEL+IMM, p=0.0070) (Figure 8A). On the other hand, tumor weights in the non-responder groups were not significantly different (Figure 8B). In addition, we found a significant increase in gene expression of COX2 (p=0.0253), IL-6 (p=0.0019), 5-HT2a (p=0.0196), CCL11 (p=0.0262), F4/80 (p=0.0310), CD80 (p=0.0103), CD206 (p=0.0023), and NCR1 (p=0.0228) in the MEL+ANE+IMM group compared to the MEL+IMM group (Figure 9).

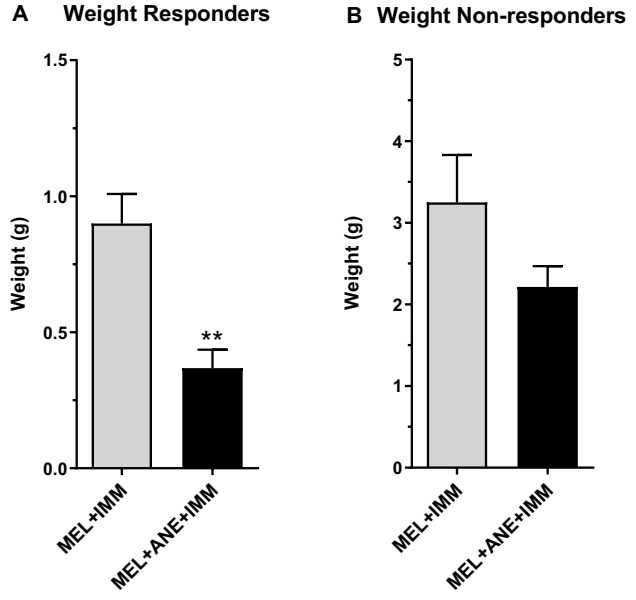

Figure 8. Tumor weights of responders and non-responders. Values are expressed as the mean ± SEM. MEL+IMM – melanoma+immunotherapy (n=8), MEL+ANE+IMM – melanoma+local anesthetics+immunotherapy (n=16). Statistical significance between groups: **p<0.01.

Discussion

We have found that topical application of the local anesthetic Pliaglis (7% lidocaine and 7% tetracaine) significantly reduced melanoma growth induced by the application of B16F0 cells. In addition, the application of Pliaglis to mice with melanoma treated with the anti-PD-1 antibody significantly enhanced the effect of this immune checkpoint inhibitor. These data suggest that the topical application of local anesthetics may be used as a neoadjuvant treatment of melanoma prior to its surgical removal.

To elucidate the mechanisms and pathways mediating the inhibitory effect of Pliaglis on melanoma growth, we used both, *in vitro* and *in vivo* approaches. First, we incubated B16F0 melanoma cells with the components of Pliaglis, lidocaine and tetracaine. We found that lidocaine or tetracaine alone dose-dependently reduced the viability of B16F0 cells. Importantly, the combination of lidocaine and tetracaine profoundly reduced cell viability even at the lowest concentrations used. In addition, we observed the same effect in the human melanoma cell line A375. These data suggest that a mixture containing the local anesthetics lidocaine and tetracaine may also be useful to suppress melanoma growth in humans.

Because the observed effect of topical application of Pliaglis on melanoma in mice may be mediated by modula-

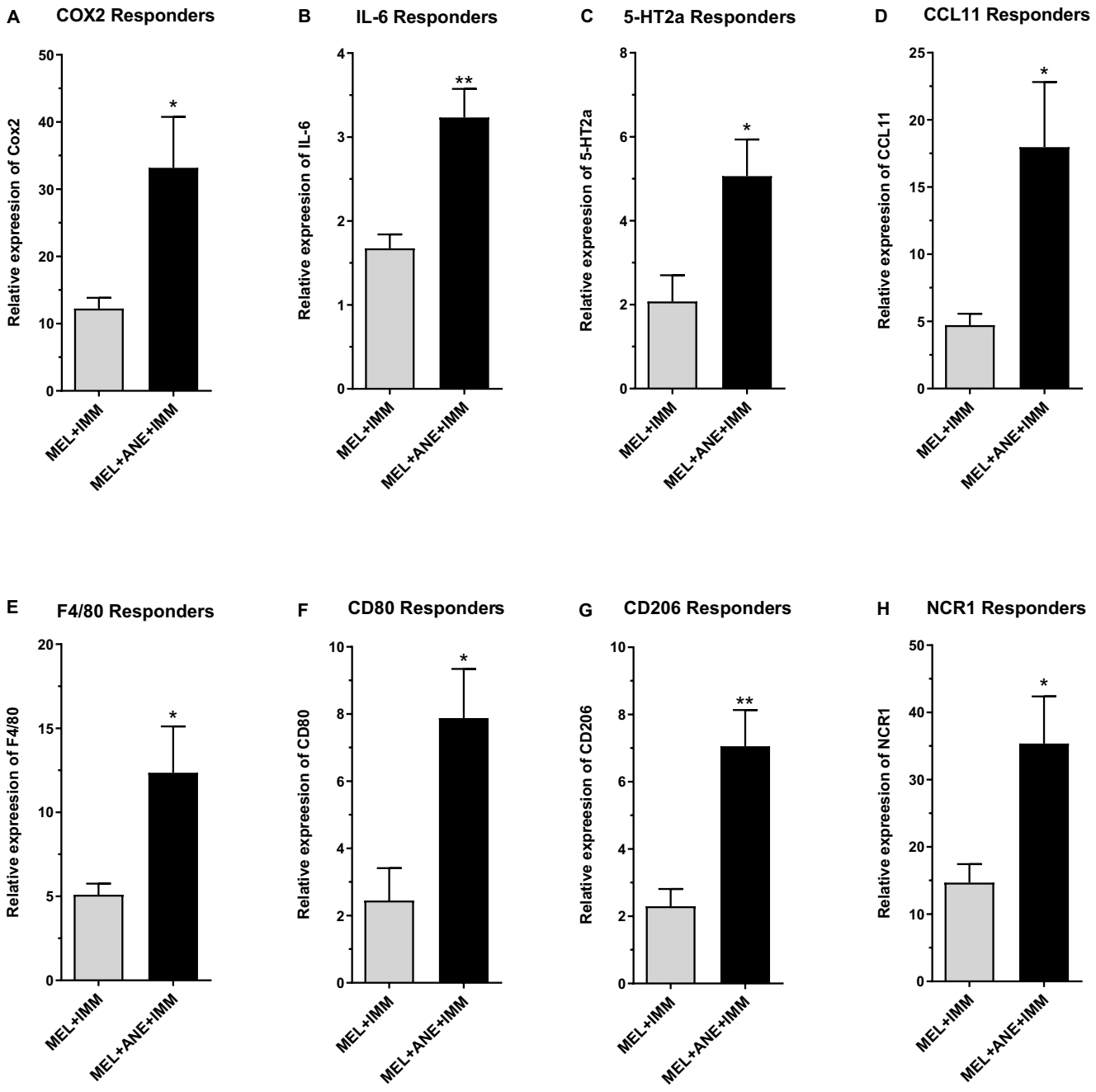

Figure 9. Gene expression of cyclooxygenase 2 (COX2) (A), interleukin 6 (IL-6) (B), 5-HT2a (C), CCL11 (D), F4/80 (E), CD80 (F), CD206 (G), and NCR1 (H) in responders. Data are presented as fold change and are used from the original chart. Values are expressed as the mean ± SEM. MEL+IMM – melanoma+immunotherapy (n=8), MEL+ANE+IMM – melanoma+local anesthetics+immunotherapy (n=16). Statistical significance between groups: *p<0.05; **p<0.01.

tion of immunity-related processes in the melanoma microenvironment, in addition to its direct effect on melanoma cells, we examined gene expression of factors related to cancer (p53), inflammation, and anticancer immunity. In addition, we determined the percentage of selected immune cell populations in melanoma tissue. Our data indicate that Pliaglis reduces the expression of p53 in mice treated with the anti-PD-1 antibody. It has been shown that the non-canonical Wnt ligand Wnt5A stabilizes the half-life of wild-type p53, which drives melanoma cells to a metastatic, therapy-resistant phenotype and initiates these cells into a slow-cycling state [15]. The increased expression of IL-1β may be responsible

for the observed effect on p53 expression, as has been shown by Qin et al. [16]. Based on these results, we suggest that local anesthetics moderately promote an antitumor microenvironment, as represented by numerous correlations with tumor weight. In addition to gene expression, we also determined the percentage of a selected population of immune cells using flow cytometry. We showed that anti-PD-1 antibody administration slightly decreased the percentage of $CD8^+Gr1^+$ memory T lymphocytes, suggesting that anti-PD-1 antibody treatment does not recruit this type of memory cells. Importantly, cytotoxic CD8 T cells expressing IFN-γ were generated exclusively from $CD8^+Gr1^+$ but not from $CD8^+Gr1^-$ T cells [10]. We also found that Pliaglis increased the number of $CD11b^+Gr1^+$, especially $CD11b^+Gr1_{high}$, but decreased the number of $CD11b^+Gr1^-$ cells. These data have to be considered in the context of the findings of Dolceti et al. [17] who showed that $CD11b^+Gr1^-$ and $CD11b^+Gr1_{int}$ subpopulations, but not $CD11b^+Gr1_{high}$ cells, are mainly responsible for the immunosuppressive effect of MDSC. Therefore, it can be suggested that the anti-tumor effect induced by Pliaglis could be potentially mediated by the reduction of immunosuppressive $CD11b^+Gr1^-$ cells to less suppressive $CD11b^+Gr1_{high}$ cells. Our findings suggest a potentially novel mechanism for the influence of sensory nerve fibers in the melanoma microenvironment, adding another piece to the puzzle similar to the findings of Balood et al. [18] who showed that a calcitonin gene-related peptide released from sensory nerve fibers increased the exhaustion of cytotoxic $CD8^+$ T cells.

Melanoma tissue is innervated by sensory and sympathetic nerve fibers and modulation of signals transmission between these nerves and the melanoma microenvironment may affect melanoma progression [19, 20]. Therefore, we also focused on the effect of Pliaglis on interactions between the nervous system and melanoma. We determined the gene expression of selected receptors for neurotransmitters and nerve growth factor and its receptor p75NTR. Administration of Pliaglis, but also anti-PD-1 antibody, reduced the expression of p75NTR, and Pliaglis modestly reduced the expression of NGF in the MEL+ANE+IMM group. Therefore, we determined the expression of MART-1 because it has been shown that NGF/p75NTR signaling reduces the expression of this melanoma-specific antigen [21]. Interestingly, in our experimental model, we found no differences in MART-1 gene expression between groups. In addition, we found increased gene expression of α9nACHR and 5-HT2a receptors after the application of Pliaglis. Interestingly, gene expression of β_2-adrenergic receptors, which are known to mediate the stimulatory effect of the sympathetic nervous system on many cancers was only affected by the anti-PD-1 antibody. Also, for this reason, it is reasonable to use a combination of β-blockers together with the anti-PD-1 antibody, as has been shown by Kokolus et al. [22].

In our experiment, we divided animals treated with anti-PD-1 antibody into responders (lower tumor weight) and non-responders (higher tumor weight). We have found that the gene expression of COX2, IL-6, 5-HT2a, CCL11, F4/80, CD80, CD206, and NCR1 was significantly increased in the MEL+ANE+IMM group compared to the MEL+IMM group. These data suggest that in responders to immune checkpoint blockade, Pliaglis promotes the expression of genes that may be responsible for the enhanced anti-tumor effect.

Clinical implications. The significant reduction in experimental melanoma growth and the significant exaggeration of the immune checkpoint inhibitor effect induced by Pliaglis suggest that the anesthetic could also be utilized in the treatment of melanoma. In support of this, we have shown that incubation of A375 human melanoma cells with compounds from Pliaglis significantly reduced cancer cell viability. As Pliaglis and other local anesthetics are approved for use in clinical practice and represent inexpensive drugs, their introduction into the oncological treatment of melanoma may be possible in the near future. Local anesthetics can be used to reduce the progression of melanoma in situations when excision of melanoma is not immediately possible. However, further research is needed to better characterize the mechanisms of action before anesthetics can be introduced into melanoma treatment.

Limitations of the study. We are aware of several limitations of the study. Although we have focused on the neurobiological aspects of melanoma, we determined the gene expression of only a few relevant receptors for neurotransmitters and nerve growth factors. The gene expression data are only descriptive and do not indicate the exact pathway that is responsible for the observed effects. Since cancer tissue is known to induce its own innervation, it will be necessary to determine the synthesis of other receptors for neurotransmitters, nerve growth factors, and molecules that attract and guide the ingrowth of new nerve fibers into cancer tissue. The further immunohistochemical study will also be necessary to visualize the presence and density and to determine the phenotype of nerve fibers innervating the melanoma tissue. Another significant limitation of our study is the relatively small sample size, therefore for a clear assessment of the effect of local anesthetic administration in the treatment of melanoma, it will be necessary to test this effect in a larger sample.

In summary, we have shown that topical application of Pliaglis significantly reduced the growth of experimental melanoma in mice. In addition, Pliaglis potentiated the efficacy of anti-PD-1 antibody. Our results suggest that this effect is mediated by a direct effect of Pliaglis on melanoma cells as well as by modulation of cancer-immune interactions. Whether the observed anti-cancer effect is also mediated by an "anesthetic" effect on the transmission of signals from peripheral nerves to cells in the melanoma microenvironment requires further investigation. Although the precise mechanisms of action are not clear, our findings suggest that local anesthetics may represent a useful tool for suppressing melanoma growth.

Supplementary information is available in the online version of the paper.

Acknowledgments: This work was supported by the Slovak Research and Development Agency (APVV-17-0090) and by a grant from Comenius University (UK/394/2023).

References

[1] MRAVEC B. Neurobiology of cancer: Definition, historical overview, and clinical implications. Cancer Med 2022; 11: 903–921. https://doi.org/10.1002/cam4.4488

[2] ONDICOVA K, MRAVEC B. Role of nervous system in cancer aetiopathogenesis. Lancet Oncol 2010; 11: 596–601. https://doi.org/10.1016/s1470-2045(09)70337-7

[3] ALBIÑANA V, GALLARDO-VARA E, CASADO-VELA J, RECIO-POVEDA L, BOTELLA LM et al. Propranolol: A „Pick and Roll" Team Player in Benign Tumors and Cancer Therapies. J Clin Med 2022; 11: 4539. https://doi.org/10.3390/jcm11154539

[4] DE GIORGI V, GRAZZINI M, BENEMEI S, MARCHIONNI N, BOTTERI E et al. Propranolol for Off-label Treatment of Patients With Melanoma: Results From a Cohort Study. JAMA Oncol 2018; 4: e172908. https://doi.org/10.1001/jamaoncol.2017.2908

[5] TILLINGER A, PADOVA A, MRAVEC B, TOMOVA A. Stressors affect urocortin 1 and urocortin 2 gene expression in rat spleen: The role of glucocorticoids. J Neuroimmunol 2019; 336: 577030. https://doi.org/10.1016/j.jneuroim.2019.577030

[6] LIVAK KJ, SCHMITTGEN TD. Analysis of relative gene expression data using real-time quantitative PCR and the 2(–Delta Delta C(T)) Method. Methods 2001; 25: 402–408. https://doi.org/10.1006/meth.2001.1262

[7] PACHYNSKI RK, SCHOLZ A, MONNIER J, BUTCHER EC, ZABEL BA. Evaluation of Tumor-infiltrating Leukocyte Subsets in a Subcutaneous Tumor Model. J Vis Exp 2015; 98: 52657. https://doi.org/10.3791/52657

[8] PAN Y, YU Y, WANG X, ZHANG T. Tumor-Associated Macrophages in Tumor Immunity. Front Immunol 2021; 12: 775758. https://doi.org/10.3389/fimmu.2021.775758

[9] MANTOVANI A, SICA A, SOZZANI S, ALLAVENA P, VECCHI A et al. The chemokine system in diverse forms of macrophage activation and polarization. Trends Immunol 2004; 25: 677–686. https://doi.org/10.1016/j.it.2004.09.015

[10] MATSUZAKI J, TSUJI T, CHAMOTO K, TAKESHIMA T, SENDO F et al. Successful elimination of memory-type CD8+ T cell subsets by the administration of anti-Gr-1 monoclonal antibody in vivo. Cell Immunol 2003; 224: 98–105. https://doi.org/10.1016/j.cellimm.2003.08.009

[11] HANNINEN A, MAKSIMOW M, ALAM C, MORGAN DJ, JALKANEN S. Ly6C supports preferential homing of central memory CD8+ T cells into lymph nodes. Eur J Immunol 2011; 41: 634–644. https://doi.org/10.1002/eji.201040760

[12] RYZHOV S, NOVITSKIY SV, GOLDSTEIN AE, BIKTASOVA A, BLACKBURN MR et al. Adenosinergic regulation of the expansion and immunosuppressive activity of CD11b+Gr1+ cells. J Immunol 2011; 187: 6120–6129. https://doi.org/10.4049/jimmunol.1101225

[13] IZOSIMOVA AV, YUZHAKOVA DV, SKATOVA VD, VOLCHKOVA LN, ZAGAINOVA EV et al. Deciphering Repertoire of B16 Melanoma Reactive TCRs by Immunization, In Vitro Restimulation and Sequencing of IFNgamma-Secreting T Cells. Int J Mol Sci 2021; 22: 9859. https://doi.org/10.3390/ijms22189859

[14] ROBERT C, RIBAS A, WOLCHOK JD, HODI FS, HAMID O et al. Anti-programmed-death-receptor-1 treatment with pembrolizumab in ipilimumab-refractory advanced melanoma: a randomised dose-comparison cohort of a phase 1 trial. The Lancet 2014; 384: 1109–1117. https://doi.org/10.1016/s0140-6736(14)60958-2

[15] WEBSTER MR, FANE ME, ALICEA GM, BASU S, KOSSENKOV AV et al. Paradoxical Role for Wild-Type p53 in Driving Therapy Resistance in Melanoma. Mol Cell 2020; 77: 633–644 e635. https://doi.org/10.1016/j.molcel.2019.11.009

[16] QIN Y, EKMEKCIOGLU S, LIU P, DUNCAN LM, LIZEE G et al. Constitutive aberrant endogenous interleukin-1 facilitates inflammation and growth in human melanoma. Mol Cancer Res 2011; 9: 1537–1550. https://doi.org/10.1158/1541-7786.MCR-11-0279

[17] DOLCETTI L, PERANZONI E, UGEL S, MARIGO I, FERNANDEZ GOMEZ A et al. Hierarchy of immunosuppressive strength among myeloid-derived suppressor cell subsets is determined by GM-CSF. Eur J Immunol 2010; 40: 22–35. https://doi.org/10.1002/eji.200939903

[18] BALOOD M, AHMADI M, EICHWALD T, AHMADI A, MAJDOUBI A et al. Nociceptor neurons affect cancer immunosurveillance. Nature 2022; 611: 405–412. https://doi.org/10.1038/s41586-022-05374-w

[19] COSTA PAC, SILVA WN, PRAZERES P, PICOLI CC, GUARDIA GDA et al. Chemogenetic modulation of sensory neurons reveals their regulating role in melanoma progression. Acta Neuropathol Commun 2021; 9: 183. https://doi.org/10.1186/s40478-021-01273-9

[20] KAMIYA A, HIYAMA T, FUJIMURA A, YOSHIKAWA S. Sympathetic and parasympathetic innervation in cancer: therapeutic implications. Clin Auton Res 2021; 31: 165–178. https://doi.org/10.1007/s10286-020-00724-y

[21] FURUTA J, INOZUME T, HARADA K, SHIMADA S. CD271 on melanoma cell is an IFN-gamma-inducible immunosuppressive factor that mediates downregulation of melanoma antigens. J Invest Dermatol 2014; 134: 1369–1377. https://doi.org/10.1038/jid.2013.490

[22] KOKOLUS KM, ZHANG Y, SIVIK JM, SCHMECK C, ZHU J et al. Beta blocker use correlates with better overall survival in metastatic melanoma patients and improves the efficacy of immunotherapies in mice. Oncoimmunology 2018; 7: e1405205. https://doi.org/10.1080/2162402X.2017.1405205

https://doi.org/10.4149/neo_2023_230418N216

Topical application of local anesthetics to melanoma increases the efficacy of the anti-PD-1 therapy

Miroslav TIBENSKY[1,2,#], Filip BLASKO[1,2,#], Peter VARGOVIC[2], Jana JAKUBIKOVA[3], Dana CHOLUJOVA[3], Jana JAKUBECHOVA[3], Boris MRAVEC[1,2,*]

Supplementary Information

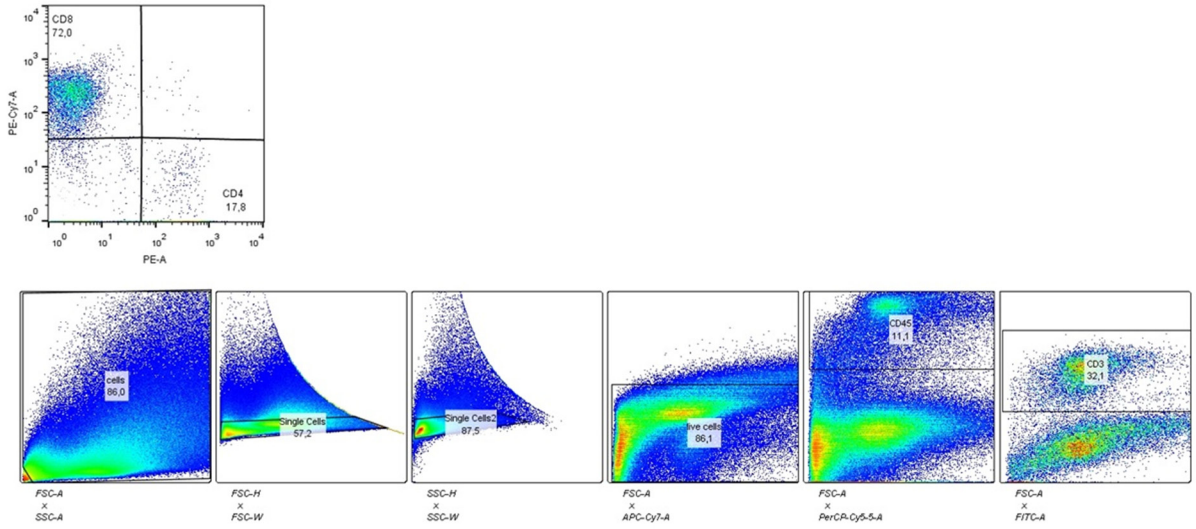

Supplementary Figure S1. Gating strategy used to identify CD4⁺ and CD8⁺ T cells. Tumors were isolated and processed into a single-cell suspension, subsequently, cells have been identified according to physical parameters and debris, doublets, and dead cells have been removed. First, immune cells via CD45 antigen have been identified and subsequently, CD3⁺ T cells have been selected, and in this CD4⁺ and CD8⁺ T cells have been recognized. Representative dot plots are hierarchically ordered.

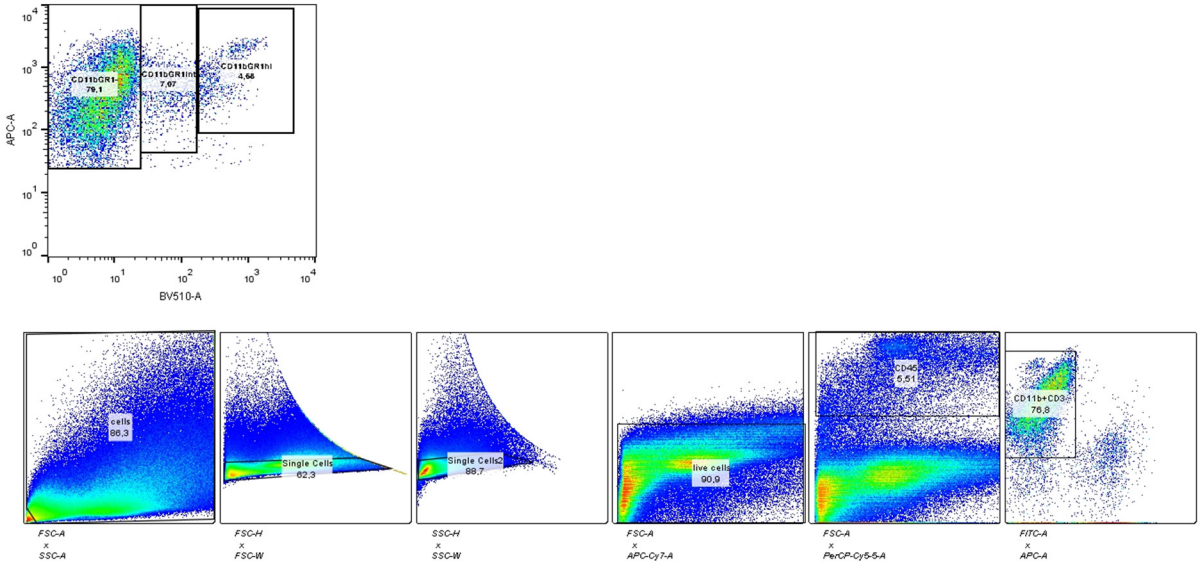

Supplementary Figure S2. Gating strategy used to identify CD11b⁺Gr1⁻, CD11b⁺Gr1$_{int}$ and CD11b⁺Gr1$_{high}$ cells. Tumors were isolated and processed into a single-cell suspension, subsequently, cells have been identified according to physical parameters and debris, doublets, and dead cells have been removed. First, immune cells via CD45 antigen have been identified and subsequently, CD11b+CD3⁻ myeloid cells have been selected, and in this CD11b⁺Gr1⁻, CD11b⁺Gr1$_{int}$ and CD11b⁺Gr1$_{high}$ cells have been recognized. Representative dot plots are hierarchically ordered.